

R-functionalized benzylphosphonic acid SAMs for improved efficiency in inverted triple cation lead perovskite solar cells

Jimmy Mangalam^a, Thomas Rath^a, Stefan Weber^a, Birgit Kunert^b, Theodoros Dimopoulos^c, Alexander Fian^d, Gregor Trimmel^a

^a Institute for Chemistry and Technology of Materials, NAWI Graz, Graz University of Technology, Stremayrgasse 9, 8010 Graz, Austria

^b Institute of Solid State Physics, Graz University of Technology, Petersgasse 16, 8010 Graz, Austria

^c AIT Austrian Institute of Technology, Center for Energy, Photovoltaic Systems, Giefinggasse 2, 1210 Vienna, Austria

^d Institute for Surface Technologies and Photonics, Joanneum Research Forschungsgesellschaft mbH

Introduction

Inverted (p-i-n) lead perovskite solar cells have reached power conversion efficiency (PCE) levels > 18% in comparison to conventional (n-i-p) perovskite solar cells with PCEs > 22% [1-3]. In order to improve the PCEs of the solar cells with inverted architecture, they are currently being investigated intensively. Among the different ideas and concepts, self assembled monolayers (SAMs) have shown promise [3]. In this study, we investigate the influence of functionalized benzylphosphonic acid SAMs (R-BPA SAMs) in a glass/ITO/NiO_x/R-BPA SAM/perovskite/PC₆₀BM/Ag solar cell setup, in which nickel oxide [4] (NiO_x) is used as a hole transport material and [6,6]-Phenyl C-61 butyric acid methyl ester (PC₆₀BM) is used as an electron transport material. We use a cesium (Cs⁺), formamidinium (FA⁺), and methylammonium (MA⁺) based triple cation perovskite as absorber layer. Benzylphosphonic acid molecules, for the modification of the NiO_x layer, were investigated including five different functional groups such as 4-bromo- (Br-), 4-fluoro- (F-), 4-nitro- (NO₂-), 4-amino- (NH₂-), and 4-methoxy- (H₃CO-).

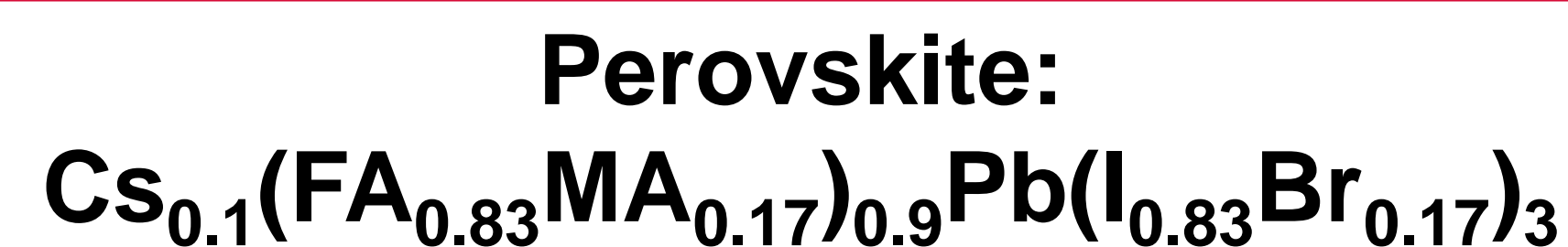
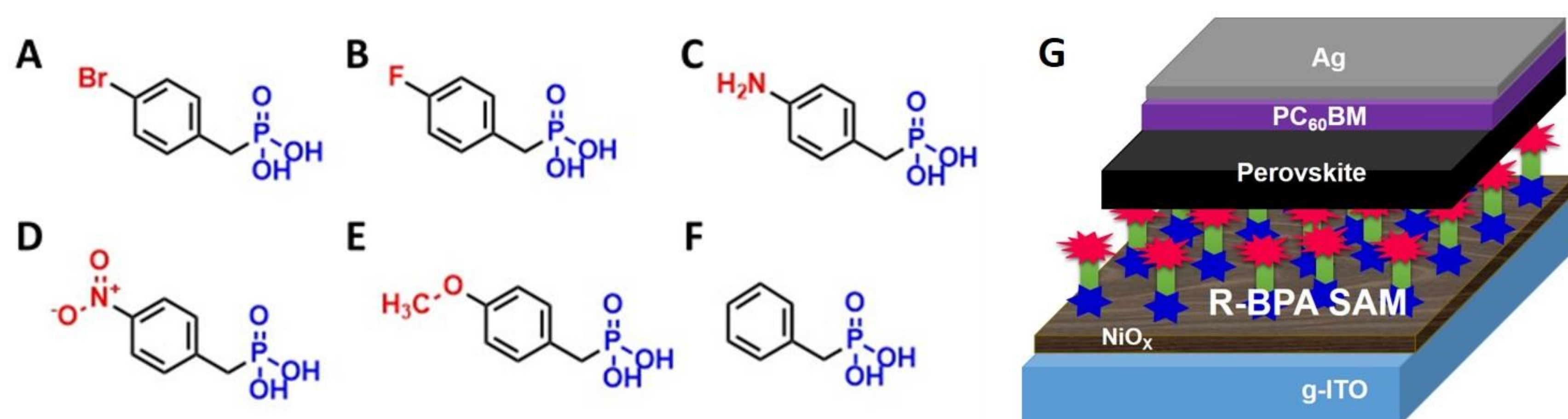


Figure 1: (A) (4-bromobenzyl)phosphonic acid, (B) (4-fluorobenzyl)phosphonic acid, (C) (4-aminobenzyl)phosphonic acid, (D) (4-nitrobenzyl)phosphonic acid, (E) (4-methoxybenzyl)phosphonic acid, (F) benzylphosphonic acid, and (G) inverted solar cell schematic with R-BPA SAM modified NiO_x film.

Characterization and results

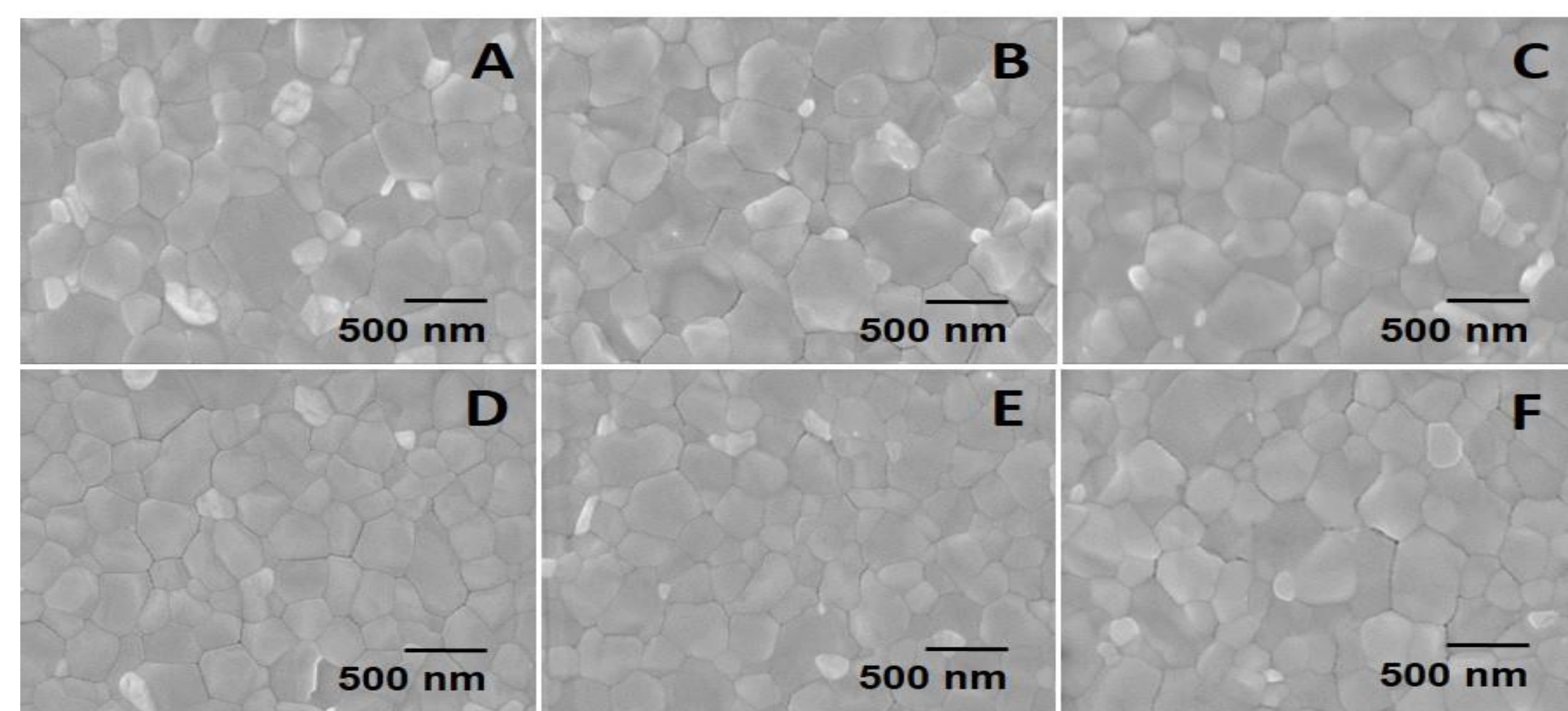
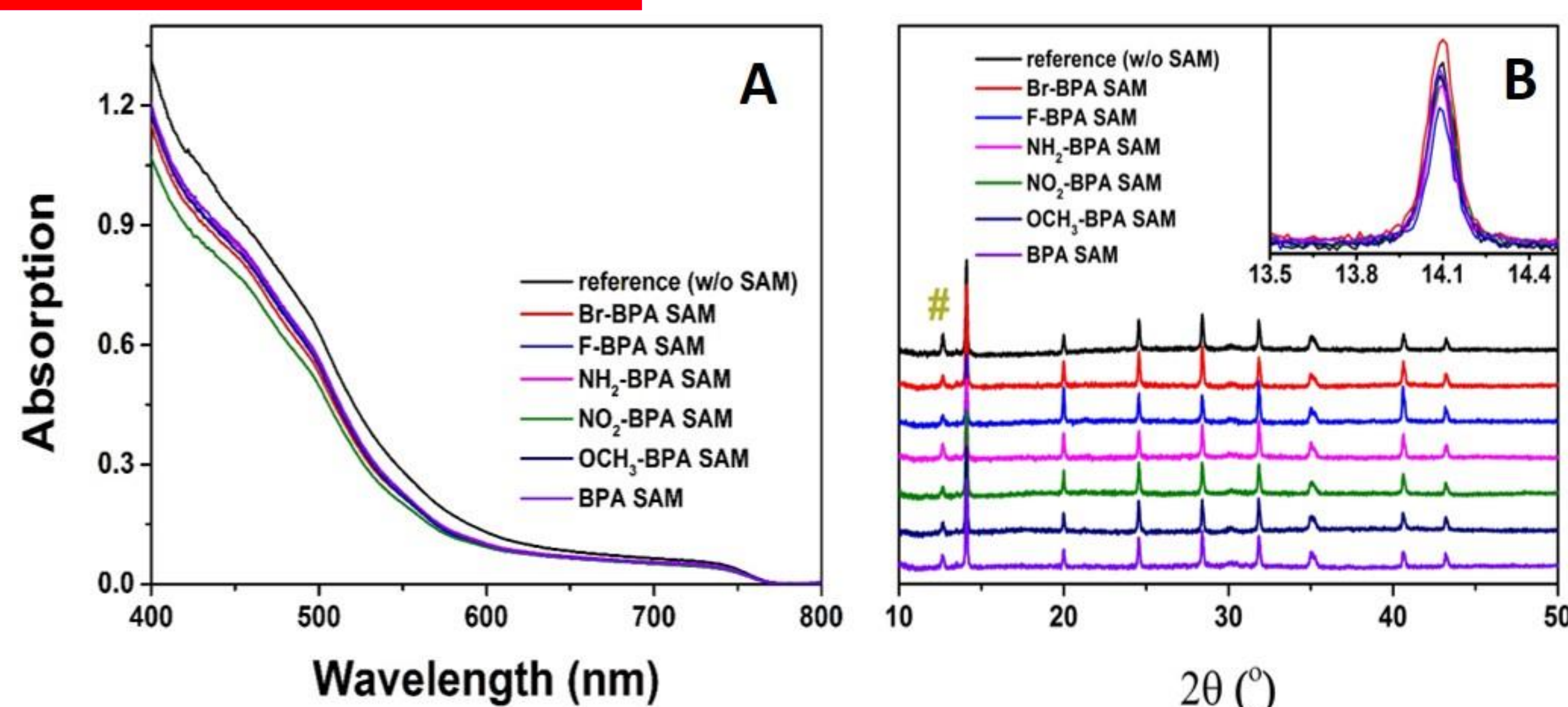


Figure 2: (A) Ultraviolet visible spectra, and (B) X-ray diffraction (XRD) patterns for glass/ITO/NiO_x/R-BPA SAM/perovskite substrate. (# represents unreacted cubic lead iodide (PbI₂) impurities.)

Figure 3: Scanning electron microscopy (SEM) images of perovskite films prepared on NiO_x films modified using (A) Br-BPA SAM, (B) F-BPA SAM, (C) NH₂-BPA, (D) NO₂-BPA SAM, (E) OCH₃-BPA SAM and (F) BPA SAM

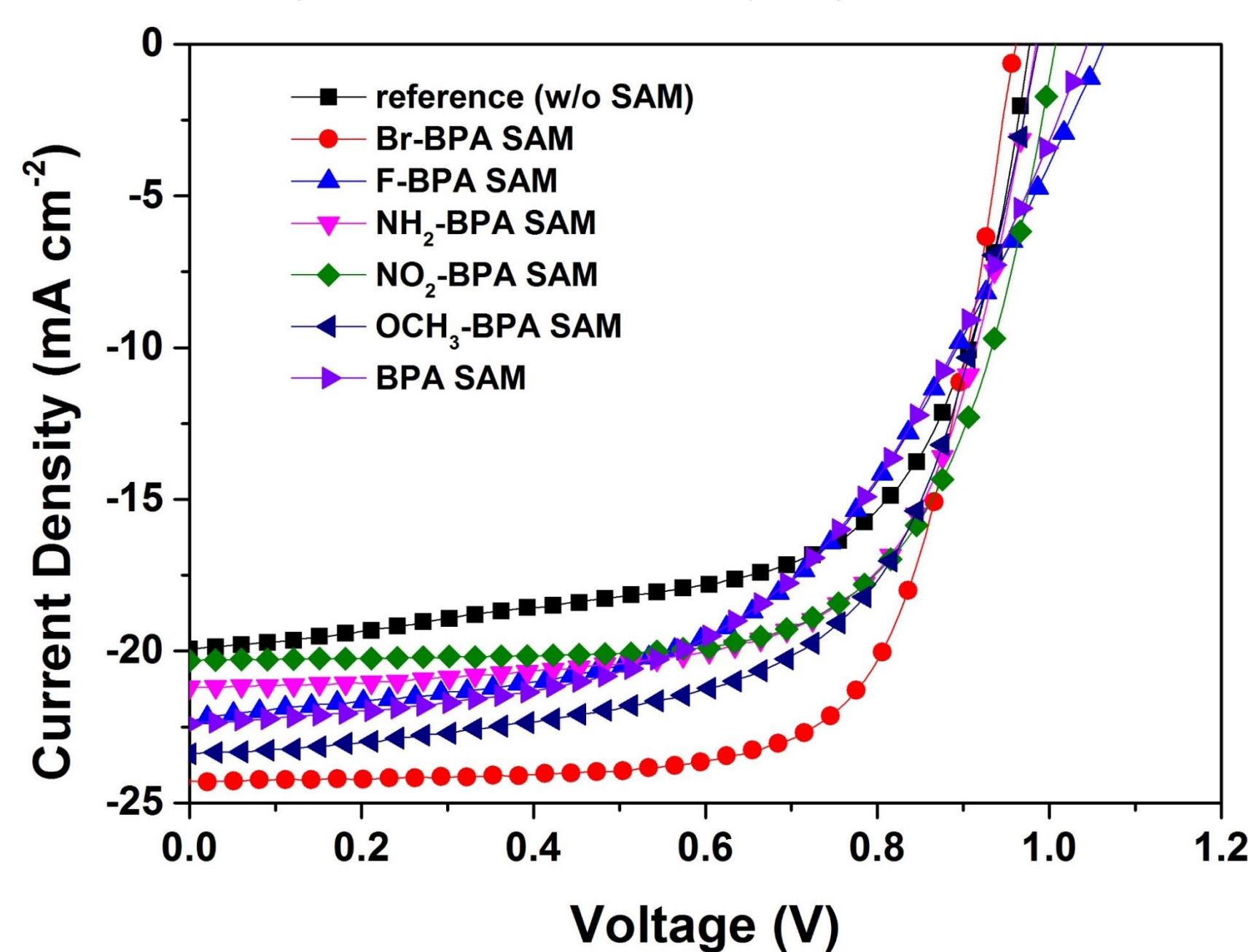


Figure 4: Current density – voltage (J-V) curves of solar cells prepared using modified NiO_x hole transport layers.

Table 1: The table enlists the PCE, open circuit voltage (V_{OC}), short circuit current density (J_{SC}) and fill factor (FF) for the solar cells represented in Figure 4.

	PCE (%)	V _{OC} (V)	J _{SC} (mA cm ⁻²)	FF
reference (w/o SAM)	12.3	0.977	-19.9	0.64
Br-BPA SAM	16.5	0.957	-24.4	0.71
F-BPA SAM	13.4	1.087	-22.5	0.54
NH ₂ -BPA SAM	13.8	0.987	-21.2	0.67
NO ₂ -BPA SAM	13.9	1.007	-20.3	0.68
OCH ₃ -BPA SAM	14.3	0.987	-23.4	0.62
BPA SAM	12.2	1.047	-22.4	0.53

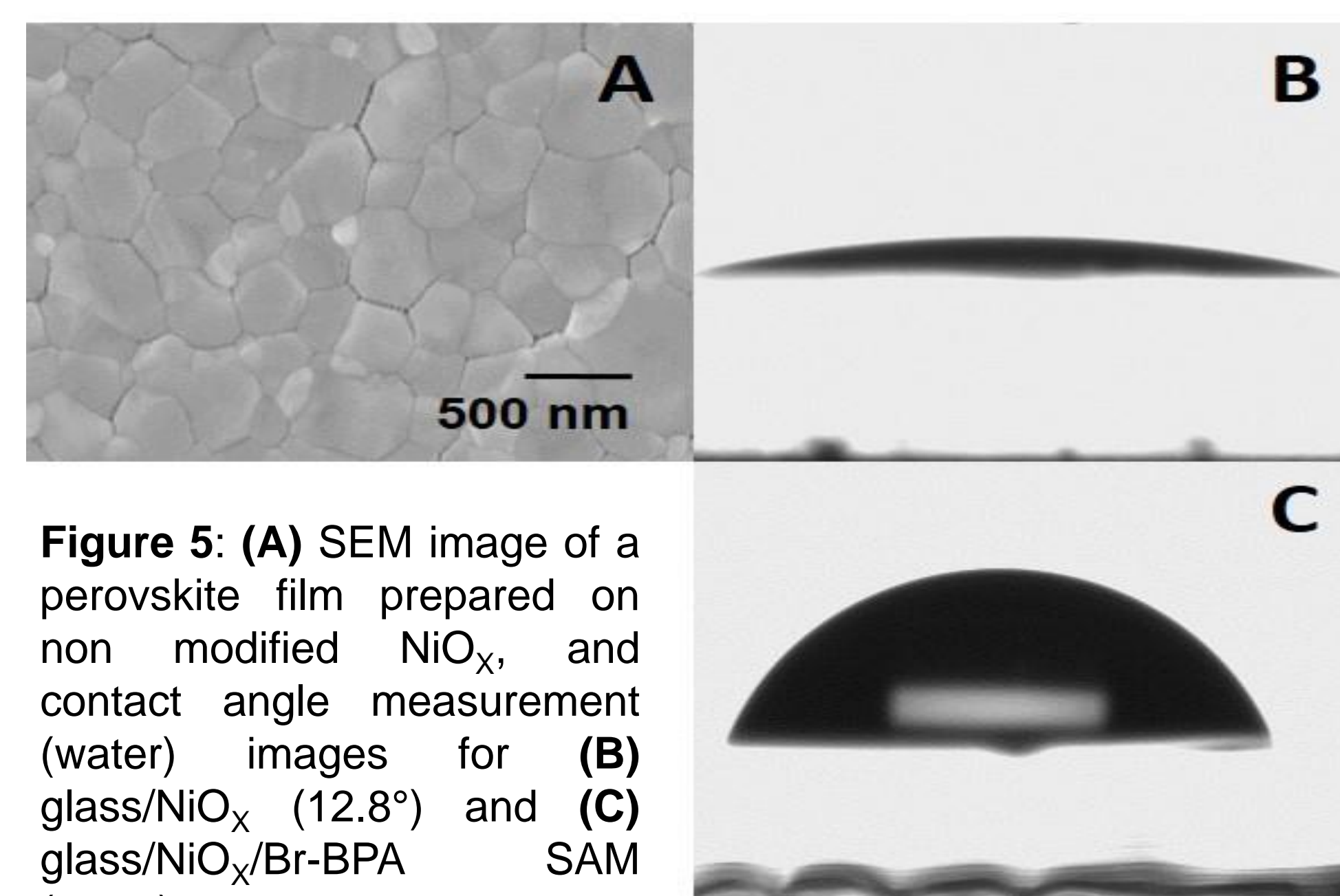


Figure 5: (A) SEM image of a perovskite film prepared on non modified NiO_x, and contact angle measurement (water) images for (B) glass/NiO_x (12.8°) and (C) glass/NiO_x/Br-BPA SAM (71.9°).

In this work, we investigated the effect of R-BPA SAMs on Cs_{0.1}(FA_{0.83}MA_{0.17})_{0.9}Pb(I_{0.83}Br_{0.17})₃ based inverted solar cells. The absorption spectra of the perovskite films prepared on the modified NiO_x films (see Figure 2A) do not reveal a change in the absorption onset of the perovskite layers. The slight difference in the absorption spectra in the lower wavelength region might stem from a slight variation in layer thickness. The X-ray diffraction patterns in Figure 2(B) show that the perovskite films crystallize in a cubic crystal structure and no significant changes in the full width half maximum of the peaks of the perovskite thin film due to the R-BPA SAMs are observed. The SEM (top view) images show smaller grain sizes and a narrower size distribution for NO₂-BPA SAM and OCH₃-BPA SAM as compared to the reference (w/o SAM) and other R-BPA SAMs as shown in Figure 3(A-F) and Figure 5(A) respectively. Figure 5(B-C) represent the contact angle measurement images for glass/NiO_x (12.8°) and glass/NiO_x/Br-BPA SAM (71.9°) using water. This indicates the presence of the Br-BPA molecules, which change the surface properties of the NiO_x layers. The J-V curves of the perovskite solar cells and the corresponding performance parameters (PCE, V_{OC}, J_{SC}, and FF) are presented in Figure 4 and Table 1, respectively. Upon introduction of the (4-bromobenzyl)phosphonic acid SAM (Br-BPA SAM), improvements in J_{SC}, V_{OC} and FF were observed. Thereby the overall performance of the solar cells increased from 11.90±1.06% (reference, average of 10 devices) to 13.65±0.81% for the Br-BPA SAM modified NiO_x hole transport layers. The champion cell with Br-BPA SAM showed a PCE of 16.5% and with the introduction of a F-BPA SAM we observed a V_{OC} of 1.087 V.

Acknowledgements

The project "FlexIPV2.0" (FFG Nr. 853 603) is funded by the Austrian "Klima und Energiefonds" within the program Energy Emission Austria. The authors thank the collaboration partners, the Austrian Institute of Technology GmbH, the Joanneum Research Forschungsgesellschaft mbH, the Crystalsol GmbH, the Linz Institute for Organic Solar Cells and the Fraunhofer Institute for Applied Polymer Research.

References

- [1] <https://www.nrel.gov/pv/assets/images/efficiency-chart.png>
- [2] M. A. Green, Y. Hishikawa, W. Warta, E. D. Dunlop, D. H. Levi, J. Hohl-Ebinger, A. W. H. Ho-Baillie, Prog. Photovolt. 2017, 25, 668–676.
- [3] Q. Wang, C. C. Chueh, T. Zhao, J. Cheng, M. Eslamian, W. C. H. Choy, A. K.-Y. Jen, ChemSusChem 2017, 10, 19, 3794–3803
- [4] S. Weber, T. Rath, J. Mangalam, B. Kunert, A. M. Coclite, M. Bauch, T. Dimopoulos, G. Trimmel, J. Mater. Sci.: Mater. Electron., 2018, 29, 3, 1847–1855